RSC Chemical Biology

ROYAL SOCIETY OF CHEMISTRY

PAPER

View Article Online
View Journal | View Issue

Cite this: *RSC Chem. Biol.*, 2024, 5, 335

A covalent compound selectively inhibits RNA demethylase ALKBH5 rather than FTO†

Gan-Qiang Lai,‡[ac] Yali Li,‡[a] Heping Zhu,‡[b] Tao Zhang,[a] Jing Gao,[a] Hu Zhou[abc] and Cai-Guang Yang*[abcd]

Received 5th December 2023,
Accepted 11th February 2024

DOI: 10.1039/d3cb00230f

rsc.li/rsc-chembio

N^6-Methyladenosine (m^6A) is the most prevalent mRNA modification and is required for gene regulation in eukaryotes. ALKBH5, an m^6A demethylase, is a promising target, particularly for anticancer drug discovery. However, the development of selective and potent inhibitors of ALKBH5 rather than FTO remains challenging. Herein, we used a targeted covalent inhibition strategy and identified a covalent inhibitor, **TD19**, which selectively inhibits ALKBH5 compared with FTO demethylase in protein-based and tumor cell-based assays. **TD19** irreversibly modifies the residues C100 and C267, preventing ALKBH5 from binding to m^6A-containing RNA. Moreover, **TD19** displays good anticancer efficacy in acute myeloid leukemia and glioblastoma multiforme cell lines. Thus, the ALKBH5 inhibitor developed in this study, which selectively targets ALKBH5 compared with FTO, can potentially be used as a probe for investigating the biological functions of RNA demethylase and as a lead compound in anticancer research.

Introduction

N^6-Methyladenosine (m^6A) is the most abundant methylation on eukaryotic mRNA;[1] it is dynamically and reversibly regulated by the m^6A methyltransferase complex (METTL3-METTL14/WTAP),[2] m^6A demethylases (fat mass and obesity-associated protein (FTO) and alkylation protein AlkB homolog 5 (ALKBH5)),[3] and m^6A binding proteins (such as YTHDF1/2/3, YTHDC1/2, IGF2BP1/2/3).[4] The m^6A modification has emerged as a key player in diverse diseases such as cancer,[5] neurodegenerative disorders,[6] and metabolic diseases;[7] it affects gene expression by regulating mRNA splicing, localization, transport, translation, and degradation.[8] ALKBH5 plays crucial roles in physiological processes in eukaryotes, including hypoxic stress and spermatogenesis.[9] Dysregulated ALKBH5 expression is associated with tumorigenesis promotion in glioblastoma stem-like cells,[10] and ALKBH5 overexpression in patients with glioblastoma multiforme (GBM) or acute myeloid leukemia (AML) is associated with poor outcomes.[11] Therefore, ALKBH5 is a potential anticancer drug target and the development of ALKBH5 inhibitors has drawn much attention in recent years.[12]

Both RNA demethylases, FTO and ALKBH5, belong to the AlkB family of nonheme Fe(II)- and 2-oxoglutarate (2OG)-dependent dioxygenases.[13] In addition, both FTO and ALKBH5 have been established as oncogenic factors that elevated the demethylation of varying methylated mRNA targets in AML and GBM tumor cells. So, either the selective inhibitors for the individual RNA demethylase or the dual inhibitors for FTO/ALKBH5 are of significant importance since they could be used as chemical probes for each RNA demethylase and drug candidates for anticancer therapies. It remains unknown whether the dual inhibitors for FTO/ALKBH5 exhibit more potent antitumor activities than the selective inhibitors. Although 2OG analogs such as **IOX3**[14] and citrate[15] and other inhibitors such as **MV1035**,[16] **ALK-04**,[17] **cmp-3**, **cmp-6**,[18] **20m**,[19] and **Ena15**,[20] generally exhibit good inhibitory activity on ALKBH5 demethylation *in vitro*, there still lacks highly selective and potent ALKBH5 inhibitors *in vivo*.[21] Moreover, the inhibitory activities of these inhibitors on tumor cells are far from satisfactory. The tumor cells treated with ALKBH5 inhibitors did not exhibit the same phenotype as ALKBH5-knockdown cells. Although the recently reported **DDO-2728** exhibited significantly improved selectivity on ALKBH5 over FTO *in vitro* and antitumor potency *in vivo*,[22] the current challenges highlight the importance of exploring alternative compounds to selectively inhibit ALKBH5.

[a] *State Key Laboratory of Drug Research, Shanghai Institute of Materia Medica, Chinese Academy of Sciences, Shanghai 201203, China. E-mail: yangcg@simm.ac.cn*
[b] *School of Pharmaceutical Science and Technology, Hangzhou Institute for Advanced Study, University of Chinese Academy of Sciences, Hangzhou 310024, China*
[c] *University of Chinese Academy of Sciences, Beijing 100049, China*
[d] *Shandong Laboratory of Yantai Drug Discovery, Bohai Rim Advanced Research Institute for Drug Discovery, Yantai 264117, China*

† Electronic supplementary information (ESI) available: Fig. S1–S6 and Tables S1, S2 and all the experimental methods. See DOI: https://doi.org/10.1039/d3cb00230f

‡ These authors contributed equally.

Targeted covalent inhibition (TCI) is an effective strategy for achieving selective enzyme modulation.[23] In this study, we identified a covalent inhibitor, **TD19**, that targets specific cysteine residues in ALKBH5 and inhibits ALKBH5 without affecting FTO. **TD19** inhibited the proliferation of both AML and GBM cell lines, underscoring its potential as a chemical tool for investigating the biological functions of ALKBH5 and as a candidate for anticancer drug in future.

Results and discussion

Tideglusib analog TD19 inhibits ALKBH5 rather than FTO

Five cysteine residues (C100, C200, C227, C230, and C267), surround the catalytic center in ALKBH5 (Fig. 1a). They are conserved across different species, such as mouse and zebrafish. However, these cysteines are not conserved in other AlkB homologs, including FTO, ALKBH2, and ALKBH3 (Fig. S1a, ESI†).[24] Interestingly, the capability for a disulfide bond formation between C230 and C267 endows ALKBH5 with the ability to distinguish single-stranded and double-stranded dm^{6}A-modified nucleic acid substrates.[15] We thus wondered whether chemically modifying these cysteines would selectively inhibit ALKBH5 without displaying off-target effects on other homologous demethylases.

We initially evaluated the inhibitory effects of iodoacetamide (**IAA**) and *N*-ethylmaleimide (**NEM**), two widely used cysteine alkylating agents, on ALKBH5 and FTO demethylation using a PAGE-based assay.[25] The nonselective RNA demethylase inhibitor **rhein** and the specific FTO inhibitor **FB23** were assayed as controls.[26] Interestingly, **NEM** (50 μM) inhibited the demethylation of dm^{6}A-modified nucleic acid substrates by ALKBH5 but not FTO, while **IAA** did not inhibit RNA demethylases (Fig. 1b). These data suggest that small-molecule modulators bearing proper electrophilic groups can selectively inhibit ALKBH5 through the chemical alkylation of cysteines. We then screened our in-house collection of covalent warhead-containing compounds on the inhibition of ALKBH5 and FTO. We found that **TD19**, an analog of **tideglusib**, whose analogs were previously identified as inhibitors of *Staphylococcus aureus* sortase A,[27] selectively inhibited ALKBH5 over FTO. **TD19** inhibited ALKBH5-induced demethylation with an IC_{50} of 1.5–3 μM while minimally inhibiting FTO and ALKBH3, even at 100 μM, as determined in the PAGE-based assay (Fig. 1c and Fig. S1b, ESI†).

To investigate the structure–activity relationship of the thiadiazolidinone scaffold of **TD19** on the inhibitory activity

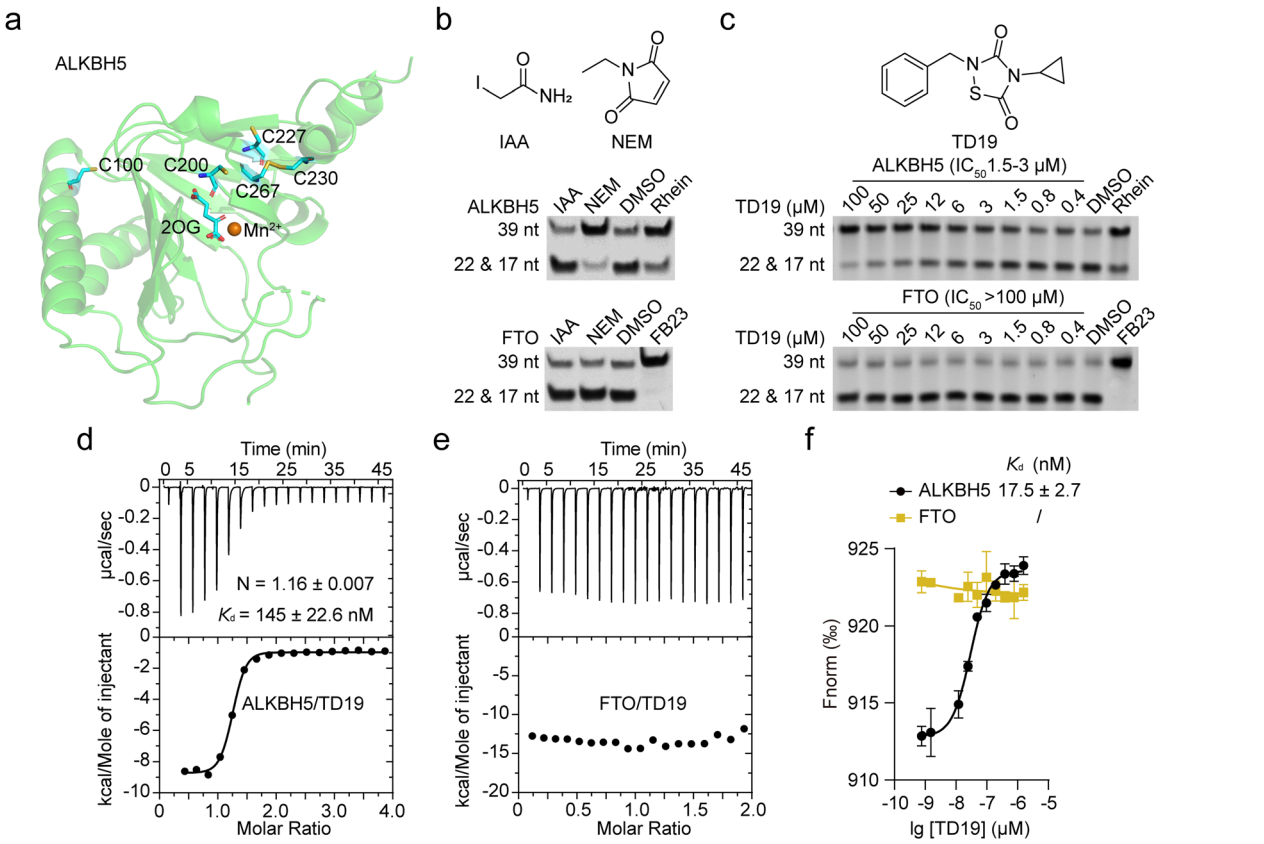

Fig. 1 **TD19** selectively inhibits ALKBH5 over FTO. (a) ALKBH5 structure (PDB ID: 4NRO) showing the five cysteines. The protein appears as green cartoon, 2OG and cysteines appear as sticks, and Mn^{2+} is the orange sphere. (b) Inhibitory effect of **IAA** and **NEM** (50 μM) on the demethylation of dm^{6}A-modified nucleic acid substrates by ALKBH5 and FTO, assessed in a PAGE-based assay. (c) Quantification of **TD19** inhibition on ALKBH5 and FTO in the PAGE-based assay. **Rhein** and **FB23** were assayed as controls. (d) and (e) Binding of **TD19** to ALKBH5 and FTO assessed by ITC titration. The dissociation constant (K_d) and stoichiometry factor (N) are indicated. (f) Binding affinity curves between **TD19** and ALKBH5 or FTO in MST assay.

toward ALKBH5, we prepared several **TD19** analogs. As shown in Table S1 (ESI†), we kept the benzyl group of **TD19** and changed the cyclopropyl to methyl, propyl, 2-chloroethyl, butyl, phenethyl, and benzyl moieties (compounds **S1–S6**, obtained in good yields). Like **TD19**, most of these analogs weakly inhibited FTO demethylation, with IC_{50} values above 50 μM. However, none of them inhibited ALKBH5 demethylation more potently than **TD19**. In addition, **S7** and **S8** analogs displayed a lower ALKBH5 demethylation inhibitory activity than **TD19** (Table S1, ESI†). Thus, we chose **TD19** to study the mode of action of this type of selective ALKBH5 inhibitor using protein binding and activity assays and tumor cell-based assays.

Next, we assessed the interaction between **TD19** and RNA demethylases. The estimated dissociation constant (K_d) of **TD19** binding to ALKBH5 was quantitatively estimated to be 145 ± 22.6 nM in an isothermal titration calorimetry (ITC) assay (Fig. 1d). Similarly, **TD19** displayed a K_d of 17.5 ± 2.7 nM for binding to ALKBH5 in a microscale thermophoresis (MST) assay (Fig. 1f). However, neither in the ITC nor MST analyses did **TD19** exhibit detectable binding to the FTO demethylase (Fig. 1e and f). These data indicate that **TD19** selectively binds to ALKBH5 compared with FTO *in vitro*.

TD19 irreversibly inhibits ALKBH5

Next, we investigated the mode of action of the selective ALKBH5 inhibitor **TD19**. We preincubated human and zebrafish ALKBH5 (referred to as fALKBH5) in the presence of **TD19** at different concentrations for various durations (0, 15, 30, and 60 min) and subsequently measured the IC_{50} values of **TD19** in a modified FRET-based m^6A detection assay (Fig. S2a, ESI†).[28] **TD19** time-dependently inhibited ALKBH5. Its IC_{50} values (after 60 min of preincubation) were 1.1 ± 0.3 μM for ALKBH5 and 0.9 ± 0.4 μM for fALKBH5 (Fig. 2a and Fig. S2b, ESI†). Next, we found that the **TD19**-induced inhibition of ALKBH5 and fALKBH5 (after 60 min of preincubation) persisted after replacing the buffer to eliminate the unbound compounds (Fig. 2b and Fig. S2c, ESI†).[29] Meanwhile, the **rhein**-induced inhibition of ALKBH5 demethylation is always time-independent and reversible (Fig. S2d, ESI†). Moreover, we observed that **TD19** reacts with endogenous thiols such as GSH in a time- and concentration-dependent manner *in vitro* (data not shown), which indicated that the cellular effects of the endogenous thiols on **TD19** should be carefully considered in future study.[30] Based on these results, we suggested that **TD19** inhibits ALKBH5 demethylation through sulfhydryl modification, similar to the RGS4 (regulator of G-protein signaling 4) inhibition mechanism by the **tideglusib** analog **CCG-50014** (Scheme 1).[31]

To assess the importance of the sulfur–nitrogen (S–N) bond in **TD19** for covalently binding to the cysteines in ALKBH5, we replaced it with a C=C bond (compound **S9**). Interestingly, **S9** completely lost its inhibitory activity toward ALKBH5, with an IC_{50} value of >50 μM (Table S2, ESI†). In addition, we prepared the S–S bond-containing compound **S10**, designed based on the ring-opening mechanism of the parental scaffold of **TD19**; this compound also showed a decreased inhibitory activity on ALKBH5 demethylation (Table S2, ESI†). These results

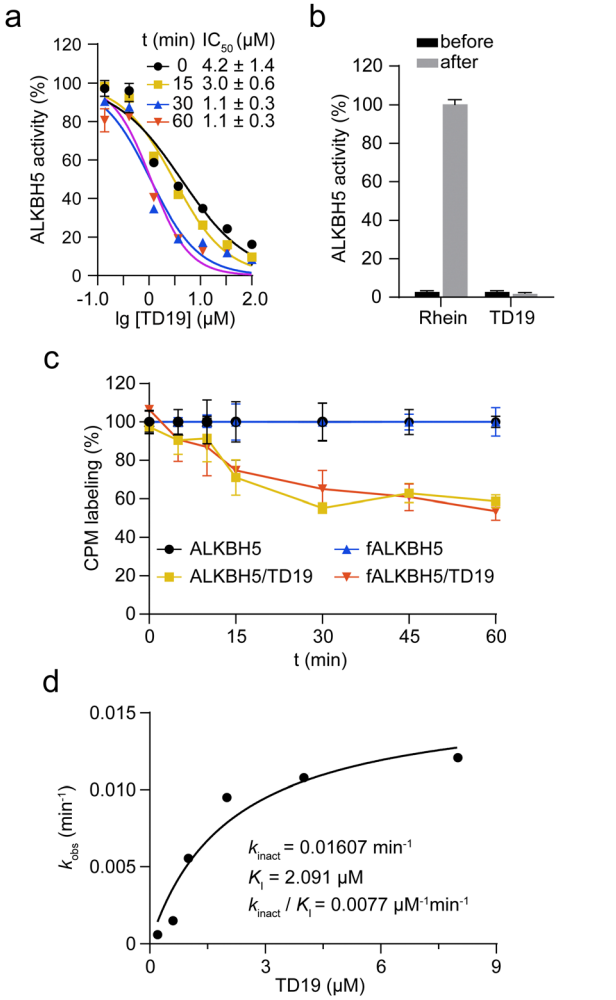

Fig. 2 **TD19** irreversibly inhibits ALKBH5. (a) Time-dependent irreversible inhibition of ALKBH5 by **TD19**, with IC_{50} values. (b) Effect of 5 μM **TD19** and 100 μM **rhein** on the demethylation by ALKBH5 in a buffer replacement assay. The control samples (treated with DMSO) were used as the 100% activity reference. (c) Quantification of the **CPM** labeling of cysteines in ALKBH5 and fALKBH5 in the presence and absence of **TD19**. (d) Kinetic analysis of the **TD19**-induced ALKBH5 inhibition in a FRET-based m^6A assay.

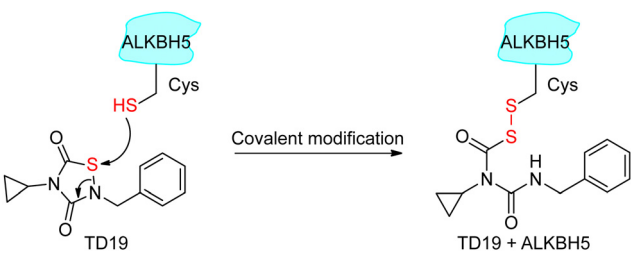

Scheme 1 Proposed reaction of **TD19** with a thiol in ALKBH5.

demonstrated that the S–N bond in **TD19** is required for the covalent inhibition of ALKBH5.

To investigate the amount of ALKBH5 cysteines affected by **TD19**, we performed a labeling assay using 7-diethylamino-3-(4-maleimidophenyl)-4-methylcoumarin (**CPM**) as a cysteine-reactive

probe.[32] The covalent addition of **TD19** to cysteine residues renders the thiol group unavailable to react with **CPM**, reducing the fluorescent signal. The fluorescence intensity of ALKBH5 pre-treated with **TD19** was around 60% of that of DMSO-treated ALKBH5, suggesting that **TD19** modified approximately two of the five cysteines around the ALKBH5 catalytic center (Fig. 2c). We also conducted a FRET-based assay to determine the inactivation constant (K_I) and maximum inactivation rate constant (k_{inact}) of **TD19**.[33] The K_I and k_{inact} values of **TD19** were 2.091 μM and 0.01607 min^{-1}, respectively, giving a k_{inact}/K_I value of 0.0077 μM^{-1} min^{-1} (Fig. 2d). These data suggest that **TD19** covalently modifies ALKBH5 in a two-step manner, with reversible binding as the first step and covalent bond formation as the second step. To evaluate the selectivity of **TD19** toward other cysteine proteases, we then evaluated the inhibitory effect of **TD19** on papain, another well-known cysteine protease.[31] We used the broad-spectrum cysteine protease inhibitor L-*trans*-epoxysuccinyl-leucylamido(4-guanidino)butane (**E64**), and the cysteine alkylator **IAA** as positive controls. **TD19** (10 μM) did not inhibit papain, whereas **E64** and **IAA** exhibited significant inhibition (Fig. S2e, ESI†), suggesting that **TD19** selectively inhibits ALKBH5 over other cysteine proteases, such as papain.

TD19 modifies C100 and C267 in ALKBH5

To scrutinize the formation of the covalent bond between **TD19** and ALKBH5, we performed mass spectrometry (MS) analysis. After treating ALKBH5 with **TD19**, we observed a higher mass peak with a mass difference of +248.53 Da, which matched the molecular weight of **TD19** (248.30 Da), indicating the covalent addition of **TD19** on ALKBH5 (Fig. 3a and b). To precisely identify the cysteine residue binding to **TD19**, we conducted HPLC-MS/MS analysis. The results revealed that **TD19** bound to either the C100 or C267 residue (Fig. 3c and d). Additionally, we analyzed the effect of **TD10** (a negative inhibitor of either ALKBH5 or FTO) on ALKBH5 using MS (Fig. S3a and b, ESI†). MS scanning revealed no additional peak in ALKBH5 treated with **TD10** (Fig. S3c, ESI†).

TD19 modification on C267 mainly contributed to the ALKBH5 inhibition

We then investigated the impact of C100 and C267 modification by **TD19** on the enzymatic inhibition of ALKBH5. An inhibition assay revealed that, after a 60-min incubation period, the IC_{50} values of **TD19** for the ALKBH5 mutants C100S, C267S, and C100SC267S were 3.2 ± 0.6 μM, 7.6 ± 3.4 μM, and 10.1 ± 3.2 μM, respectively (Fig. 4a–c). This result suggests that **TD19** retains its binding affinity with cysteine mutants and demonstrates inhibitory activity. Furthermore, the modification of **TD19** on C267 contributes more to the inhibitory effect than that on C100. Similarly, **TD19** displayed reduced inhibitory effects on the corresponding mutants of fALKBH5 (where C68 and C235 in fALKBH5 correspond to C100 and C267 in ALKBH5, respectively), further underscoring the mechanism of **TD19** modification on C100 and C267 residues in ALKBH5 (Fig. S4a, ESI†).

Next, we performed an MST assay to determine the binding stoichiometry of **TD19** and ALKBH5 mutants. The K_d values between **TD19** and the ALKBH5 mutants C100S, C267S, and C100SC267S were 185 ± 33, 1526 ± 424, and 1714 ± 221 nM, respectively (Fig. 4d). In addition, we quantified the K_d values for the binding of **TD19** to the ALKBH5 mutants C100S, C267S,

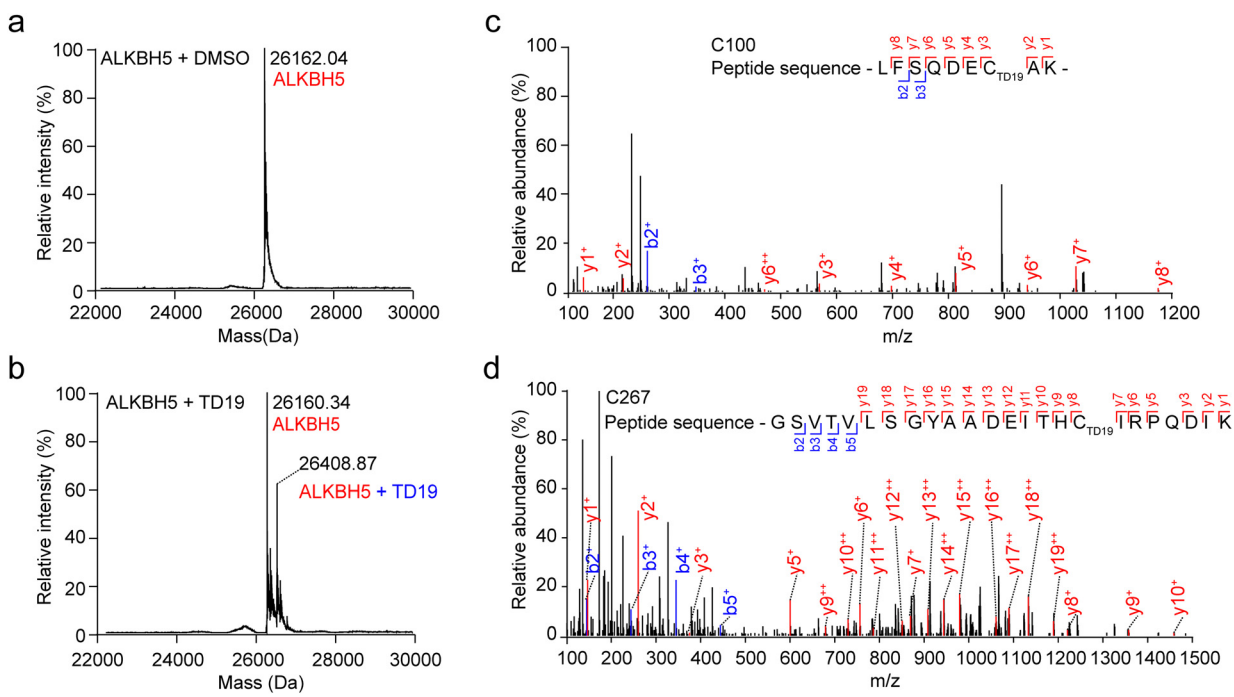

Fig. 3 Identification of the modification sites of **TD19** in ALKBH5. (a) and (b) Mass spectrometry spectra of ALKBH5 incubated with DMSO or **TD19**. (c) and (d) HPLC-MS/MS results indicating that **TD19** modified C100 and C267 in ALKBH5.

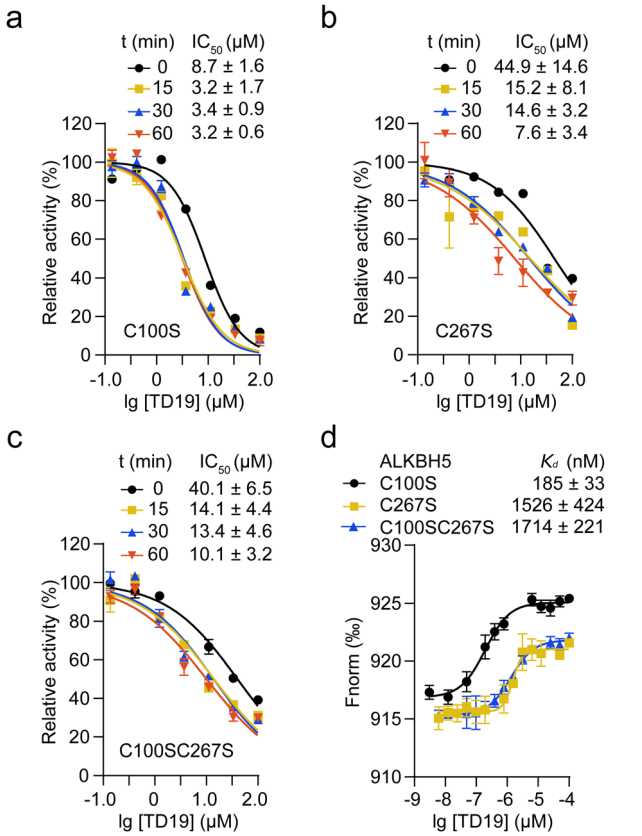

Fig. 4 Effect of cysteine mutations on the inhibition of ALKBH5 by **TD19**. (a)–(c) Inhibition of **TD19** on the ALKBH5 mutants C100S, C267S, and C100SC267S after different incubation times. (d) Binding affinity between **TD19** and the ALKBH5 mutants by MST assay.

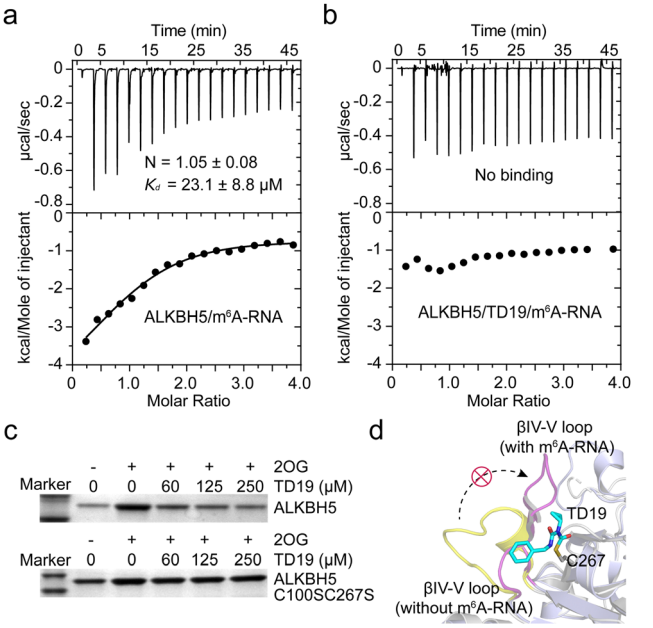

Fig. 5 Effect of **TD19** on the interaction between ALKBH5 and substrate. (a) and (b) Effect of **TD19** on the binding of ALKBH5 with an m^{6}A-RNA substrate in ITC titration. (c) Effect of **TD19** on the interaction between dm^{6}A-containing DNA oligonucleotide and ALKBH5 WT and the C100SC267S mutant in a pull-down assay. (d) Structural superimposition of the ALKBH5/m^{6}A-RNA complex structure (light blue cartoon, PDB ID: 7WKV) and the apo structure of ALKBH5 (white cartoon, PDB ID: 4NRO). **TD19** (colored in cyan) was docked with C267 of the apo ALKBH5 structure. The βIV-V loops with and without the m^{6}A-RNA substrate were colored in purple and yellow, respectively.

and C100SC267S as 335 ± 68, 825 ± 209, and 1110 ± 260 nM, respectively, *via* an ITC assay. (Fig. S4b–d, ESI†). These results suggest that the modification of **TD19** on C267 contributes more to the binding capacity of **TD19** toward ALKBH5 than that on C100. Additionally, we estimated the stoichiometry factor (N) of **TD19** titration to the C100SC267S mutant to be 0.74 ± 0.02 by ITC assay, indicating that **TD19** still bound to ALKBH5 in the absence of the two cysteine residues. This observation suggests that **TD19** covalently modifies ALKBH5 in a two-step manner, consistent with previous findings (Fig. 2d).

TD19 inhibits ALKBH5 binding to m^{6}A-RNA substrate

To investigate the mechanism of ALKBH5 inhibition by **TD19**, we determined the K_d values for ALKBH5 and the m^{6}A-containing RNA substrate in the presence and absence of **TD19** in an ITC assay.[34] Without **TD19**, ALKBH5 bound to m^{6}A-RNA with a K_d of 23.1 ± 8.8 μM (Fig. 5a). However, no binding was detected when ALKBH5 was preincubated with **TD19** (Fig. 5b). In addition, we conducted a pull-down assay to evaluate the effect of **TD19** on the interaction between ALKBH5 and a dm^{6}A-containing DNA substrate as previously described.[35] ALKBH5 is known to weakly bind to DNA substrates in the absence of 2OG. Therefore, we assayed the sample without 2OG as the control. **TD19** inhibited the binding between ALKBH5 and the DNA substrate in a concentration-dependent manner, but minimally disrupted the C100SC267S mutant binding to the DNA substrate (Fig. 5c). These data show that the modification of ALKBH5 by **TD19** inhibits RNA demethylase binding to the methylated RNA/DNA substrate.

To investigate the potential interaction mode between **TD19** and ALKBH5, we conducted a docking study using the reported ALKBH5 structure as a model.[15] In the covalent docking model of **TD19** and C100 in ALKBH5, two hydrogen bonds were observed (Fig. S5a and b, ESI†). One is formed between the carbonyl group in **TD19** and the –NH of Arg93, with a distance of 3.2 Å, the other is formed between the –NH in **TD19** and the carbonyl group of Arg250, with a distance of 3.4 Å. In the covalent docking model of **TD19** and C267 in ALKBH5, a hydrogen bond was observed between the carbonyl group in **TD19** and the –NH in the Gln233 residue, with a distance of 2.6 Å (Fig. S5c and d, ESI†). Additionally, the phenyl ring of **TD19** forms a π–π stacking interaction with Phe232 (Fig. S5c, ESI†). Next, we performed a superimposition of the ALKBH5/m^{6}A-RNA complex and the apo ALKBH5 structure and found that the βIV-V loop (residues 229–242) underwent a large conformational change in the ALKBH5/m^{6}A-RNA complex compared to the apo ALKBH5 structure. The docking model suggested that **TD19** modification on C267 hindered the conformational change in the βIV-V loop, potentially impeding ALKBH5 binding to the methylated RNA substrate (Fig. 5d).

Nevertheless, resolving the structure of the **TD19**/ALKBH5 complex would give more precise insights on mode of action of **TD19**.

TD19 targets ALKBH5 and regulates the cellular m^{6}A for anticancer

ALKBH5 is required for tumor growth in AML[11] and GBM.[10] To assess the anticancer potential of **TD19**, we evaluated its effect on the viability of two AML (NB4 and MOLM13) and two GBM cell lines (U87 and A172), using **FB23-2** as a control **TD19** exhibited good antiproliferative effects on all four tumor cell lines in a dose-dependent manner. The IC_{50} values were 15.1 ± 1.4, 9.5 ± 3.0, 7.2 ± 0.4, and 22.3 ± 1.7 μM in the NB4, MOLM13, U87, and A172 cell lines, respectively (Fig. 6a). The FTO inhibitor **FB23-2** displayed better activities than **TD19** (Fig. S6a, ESI†). To corroborate the direct interaction between **TD19** and ALKBH5 in cells, we conducted a drug affinity responsive target stability (DARTS) assay. As expected, the presence of **TD19** in NB4 and U87 cells rendered ALKBH5, but not FTO, resistant to protease hydrolysis (Fig. 6b), suggesting that **TD19** directly and selectively targeted ALKBH5 in cell lysates. We also evaluated the effect of **TD19** on the m^{6}A modification in tumor cell lines. The treatment with **TD19** increased m^{6}A levels in NB4, MOLM13, U87, and A172 cells, as detected through an m^{6}A dot blot assay (Fig. 6c, and Fig. S6b, ESI†). Conversely, treating the cells with the negative control compound **TD10** minimally altered m^{6}A levels (Fig. 6d and Fig. S6c, ESI†). The abundance of the m^{1}A modification in NB4 and U87 cells remained unchanged upon treatment with **TD19**, showing that **TD19** did not inhibit ALKBH3-mediated m^{1}A demethylation in tumor cells (Fig. 6e).

We also investigated the target engagement of **TD19** in tumor cells. We constructed stable cell lines with decreased ALKBH5 mRNA expression by utilizing two short hairpin RNAs (shA5-1 and shA5-2, collectively referred to as shALKBH5) (Fig. 6f). Compared with the control shRNA (referred to as shNC), shALKBH5 significantly increased the m^{6}A abundance detected by dot blot assay in NB4 and U87 cells (Fig. 6f). Interestingly, **TD19** treatment minimally affected m^{6}A levels in shALKBH5-treated cells, implying that **TD19** regulates cellular m^{6}A levels in an ALKBH5-dependent manner (Fig. 6f and Fig. S6d, ESI†). Moreover, **TD19** at 10–20 μM exhibited a significantly lower inhibitory effect on the viability of shALKBH5-treated AML and GBM cells than on shNC-treated ones, implying that the **TD19** inhibition of cell proliferation is contingent on ALKBH5 protein levels (Fig. 6g). To further evaluate the on-target effects of **TD19** on the regulation of m^{6}A abundance in tumor cells, we transfected NB4 and U87

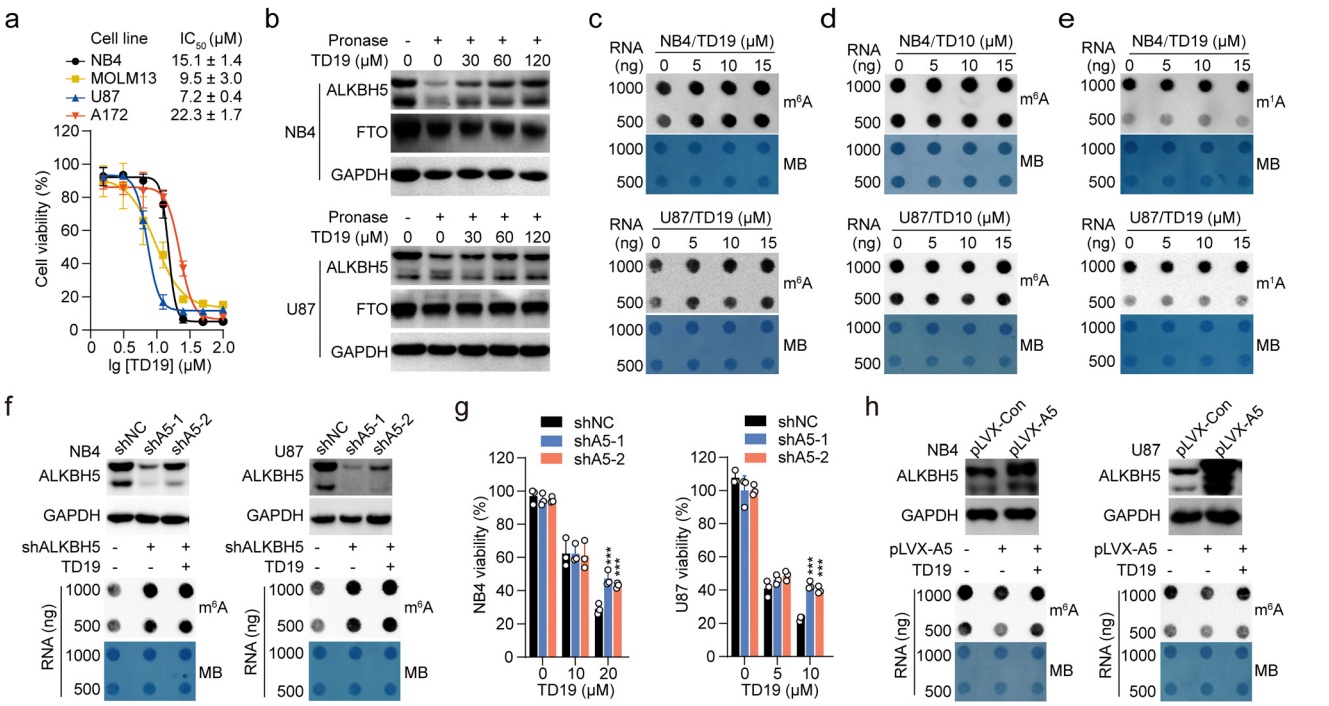

Fig. 6 **TD19** regulates m^{6}A modification and shows anticancer activity in tumor cells. (a) Effect of **TD19** on the viability of AML and GBM cells. The cells were treated with **TD19** for 72 h at the indicated concentrations before MTT/CCK8 measurement. (b) Representative gel images showing the effect of **TD19** on the hydrolysis of ALKBH5 and FTO by pronase in the DARTS assay. The ALKBH5 and FTO levels in NB4 and U87 cells were quantified by western blot. (c) and (d) Effect of **TD19** (c) and **TD10** (d) on m^{6}A abundance in NB4 and U87 cells. The cells were treated with the compounds for 72 h before quantification of m^{6}A in total RNA through a dot blot assay. Methylene blue was used as a loading control for RNA samples. (e) Effect of **TD19** on m^{1}A abundance in NB4 and U87 cells, assessed by dot blot assay. (f) Effect of **TD19** on m^{6}A abundance in ALKBH5 knockdown NB4 and U87 cells, assessed through an m^{6}A dot blot assay. (g) Effect of **TD19** on the viability of ALKBH5 knockdown NB4 and U87 cells. The cells were treated with **TD19** for 72 h. (h) Effect of **TD19** on m^{6}A abundance in NB4 and U87 cells overexpressing ALKBH5, assessed through an m^{6}A dot blot assay. Statistical significance is denoted as ***$p < 0.001$ using the unpaired Student's t-test. The error bars represent the mean ± SD, $n = 3$.

cells using lentiviruses containing a wild-type ALKBH5 plasmid (referred to as pLVX-A5). This transfection significantly reduced the m^{6}A level in the tumor cells. However, **TD19** treatment counteracted the decrease of the m^{6}A abundance resulting from ALKBH5 overexpression (Fig. 6h). Collectively, these results indicate that the regulation of m^{6}A by **TD19** is dependent on ALKBH5 in tumor cells.

Lastly, we investigated whether **TD19** treatment regulated the expression of downstream target genes of ALKBH5 using real-time quantitative polymerase chain reaction (RT-qPCR). Two direct target genes, AXL (AXL receptor tyrosine kinase) in AML and FOXM1 (Forkhead box M1) in GBM, which promote tumorigenesis, were selected for validation. In line with the positive regulation of AXL and FOXM1 expression by ALKBH5 in AML and GBM cells, treatment with **TD19** or shALKBH5 significantly reduced the mRNA abundance of the two genes (Fig. S6e and f5, ESI†). These findings show that **TD19** targets ALKBH5 and regulates the mRNA expression of downstream genes.

Conclusions

ALKBH5 and FTO are the two known m^{6}A demethylases in RNA epigenetics. They are usually highly expressed in AML and GBM tumor cells. Overexpression of m^{6}A demethylases is associated with poor outcomes in patients with these diseases. These results highlight the therapeutic significance for the development of small-molecule inhibitors that selectively targets certain m^{6}A demethylase because FTO and ALKBH5 are homologous demethylases.[36] The development of selective FTO inhibitors by us and others has greatly progressed,[37] while the development of selective and highly potent inhibitors for ALKBH5 remains challenging.

Our identification of **TD19** as a covalent and selective inhibitor for ALKBH5 rather than FTO has revealed a general path to the selective inhibition of ALKBH5 by covalent modification on cysteines using an established TCI strategy. Although several crystal structures of the apo ALKBH5 protein and the ALKBH5/substrate complex have been resolved, the structure-guided development of selective ALKBH5 inhibitors has made little progress. The highly conserved ligand binding pockets shared by the ALKBH5 and FTO demethylases easily explain the slow development of highly selective ALKBH5 inhibitors. Inspired by the unexpected observation of the covalent modification of **IOX3** on C200 in the crystal structure of ALKBH5, we wondered whether the cysteine residues near the substrate binding site could serve as covalent modification sites for the selective inhibition of ALKBH5 over other non-heme Fe(II)/2OG-dependent demethylases. Interestingly, the commercially available alkylating agent **NEM** selectively inhibited the demethylation of ALKBH5 but not FTO, supporting the idea of covalent modification on cysteines for the selective inhibition of ALKBH5. We then showed that **TD19** covalently bound to the C100 and C267 ALKBH5 residues, disrupting the binding between ALKBH5 and m^{6}A-RNA substrates, thus selectively inhibiting ALKBH5 demethylation over FTO, and modulating m^{6}A levels and downstream genes expression in AML and GBM tumor cell lines.

We are aware that demonstrating the chemical traceability of the active cysteines in ALKBH5 in the cellular environment is warranted. It is required to develop highly selective covalent inhibitors of ALKBH5 with minimal off-target effects, which might be caused by the nonselective modification on undesired cysteines. The substantiation of this validation necessitates the systematic profiling of cysteine activity and accessibility within ALKBH5, a task well-suited to the application of chemical proteomics methodologies, notably activity-based protein profiling.[38] In addition, a large-scale high-throughput screening of the covalent compound library would provide more hit scaffolds for synthesis optimization. Furthermore, we acknowledge the necessity for additional investigation to intricately dissect the selectivity of **TD19** against a comprehensive array of pharmacologically relevant targets, encompassing GSK3β, the target of the related inhibitor **tideglusib**.[39]

In summary, our findings establish **TD19** as a selective and potent covalent inhibitor of ALKBH5 that effectively interferes with m^{6}A regulation in tumor cells. **TD19** is a promising chemical tool to explore ALKBH5 functions and a starting point for developing anticancer drug candidates selectively targeting ALKBH5 rather than FTO.

Author contributions

C.-G.Y. conceptualization, project administration, writing – original draft, writing – review & editing, funding acquisition. G.-Q.L., H.Z. data curation, validation, methodology, writing – original draft, writing – review & editing. Y.L. data curation, validation, methodology, writing – original draft, writing – review & editing, funding acquisition. T.Z., J.G., H.Z. data curation.

Conflicts of interest

There are no conflicts to declare.

Acknowledgements

We thank the staff of the Large-scale Protein Preparation System at the National Facility for Protein Science (NFPS) in Shanghai, Shanghai Advanced Research Institute, Chinese Academy of Sciences, China for providing technical support and assistance in data collection and analysis of ITC and MST assays. This work was supported by the National Natural Science Foundation of China (22007093 to Y. L. and 92153303 to C.-G. Y.), the National Key Research and Development Program of China (2022YFC2705005 to C.-G. Y.).

Notes and references

1 C. He, *Nat. Chem. Biol.*, 2010, **6**, 863–865; I. A. Roundtree, M. E. Evans, T. Pan and C. He, *Cell*, 2017, **169**, 1187–1200.

2 J. Liu, Y. Yue, D. Han, X. Wang, Y. Fu, L. Zhang, G. Jia, M. Yu, Z. Lu, X. Deng, Q. Dai, W. Chen and C. He, *Nat. Chem. Biol.*, 2014, **10**, 93–95; L. Lan, Y. J. Sun, X. Y. Jin, L. J. Xie, L. Liu and L. Cheng, *Angew. Chem., Int. Ed.*, 2021, **60**, 18116–18121.
3 G. F. Jia, Y. Fu, X. Zhao, Q. Dai, G. Q. Zheng, Y. Yang, C. Q. Yi, T. Lindahl, T. Pan, Y. G. Yang and C. He, *Nat. Chem. Biol.*, 2011, **7**, 885–887; G. Zheng, J. A. Dahl, Y. Niu, P. Fedorcsak, C. M. Huang, C. J. Li, C. B. Vågbø, Y. Shi, W. L. Wang, S. H. Song, Z. Lu, R. P. G. Bosmans, Q. Dai, Y. J. Hao, X. Yang, W. M. Zhao, W. M. Tong, X. J. Wang, F. Bogdan, K. Furu, Y. Fu, G. Jia, X. Zhao, J. Liu, H. E. Krokan, A. Klungland, Y. G. Yang and C. He, *Mol. Cell*, 2013, **49**, 18–29.
4 Z. Zou, C. Sepich-Poore, X. Zhou, J. Wei and C. He, *Genome Biol.*, 2023, **24**, 17.
5 Y. Huang, R. Su, Y. Sheng, L. Dong, Z. Dong, H. Xu, T. Ni, Z. S. Zhang, T. Zhang, C. Li, L. Han, Z. Zhu, F. Lian, J. Wei, Q. Deng, Y. Wang, M. Wunderlich, Z. Gao, G. Pan, D. Zhong, H. Zhou, N. Zhang, J. Gan, H. Jiang, J. C. Mulloy, Z. Qian, J. Chen and C.-G. Yang, *Cancer Cell*, 2019, **35**, 677–691.
6 R. Castro-Hernández, T. Berulava, M. Metelova, R. Epple, T. Peña Centeno, J. Richter, L. Kaurani, R. Pradhan, M. S. Sakib, S. Burkhardt, M. Ninov, K. E. Bohnsack, M. T. Bohnsack, I. Delalle and A. Fischer, *Proc. Natl. Acad. Sci. U. S. A.*, 2023, **120**, e2204933120.
7 B. Zhang, H. Jiang, Z. Dong, A. Sun and J. Ge, *Genes Dis.*, 2021, **8**, 746–758.
8 H. Shi, J. Wei and C. He, *Mol. Cell*, 2019, **74**, 640–650.
9 A. Thalhammer, Z. Bencokova, R. Poole, C. Loenarz, J. Adam, L. O'Flaherty, J. Schödel, D. Mole, K. Giaslakiotis, C. J. Schofield, E. M. Hammond, P. J. Ratcliffe and P. J. Pollard, *PLoS One*, 2011, **6**, e16210.
10 S. Zhang, B. S. Zhao, A. Zhou, K. Lin, S. Zheng, Z. Lu, Y. Chen, E. P. Sulman, K. Xie, O. Bögler, S. Majumder, C. He and S. Huang, *Cancer Cell*, 2017, **31**, 591–606.
11 J. Wang, Y. Li, P. Wang, G. Han, T. Zhang, J. Chang, R. Yin, Y. Shan, J. Wen, X. Xie, M. Feng, Q. Wang, J. Hu, Y. Cheng, T. Zhang, Y. Li, Z. Gao, C. Guo, J. Wang, J. Liang, M. Cui, K. Gao, J. Chai, W. Liu, H. Cheng, L. Li, F. Zhou, L. Liu, Y. Luo, S. Li and H. Zhang, *Cell Stem Cell*, 2020, **27**, 81–97; C. Shen, Y. Sheng, A. C. Zhu, S. Robinson, X. Jiang, L. Dong, H. Chen, R. Su, Z. Yin, W. Li, X. Deng, Y. Chen, Y. C. Hu, H. Weng, H. Huang, E. Prince, C. R. Cogle, M. Sun, B. Zhang, C. W. Chen, G. Marcucci, C. He, Z. Qian and J. Chen, *Cell Stem Cell*, 2020, **27**, 64–80.
12 D. Shen, B. Wang, Y. Gao, L. Zhao, Y. Bi, J. Zhang, N. Wang, H. Kang, J. Pang, Y. Liu, L. Pang, Z. S. Chen, Y. C. Zheng and H. M. Liu, *Acta Pharm. Sin. B*, 2022, **12**, 2193–2205.
13 M. A. Kurowski, A. S. Bhagwat, G. Papaj and J. M. Bujnicki, *BMC Genomics*, 2003, **4**, 48.
14 W. Aik, J. S. Scotti, H. Choi, L. Gong, M. Demetriades, C. J. Schofield and M. A. McDonough, *Nucleic Acids Res.*, 2014, **42**, 4741–4754.
15 C. Feng, Y. Liu, G. Wang, Z. Deng, Q. Zhang, W. Wu, Y. Tong, C. Cheng and Z. Chen, *J. Biol. Chem.*, 2014, **289**, 11571–11583.
16 A. Malacrida, M. Rivara, A. Di Domizio, G. Cislaghi, M. Miloso, V. Zuliani and G. Nicolini, *Bioorg. Med. Chem.*, 2020, **28**, 115300.
17 N. Li, Y. Kang, L. Wang, S. Huff, R. Tang, H. Hui, K. Agrawal, G. M. Gonzalez, Y. Wang, S. P. Patel and T. M. Rana, *Proc. Natl. Acad. Sci. U. S. A.*, 2020, **117**, 20159–20170.
18 S. Selberg, N. Seli, E. Kankuri and M. Karelson, *ACS Omega*, 2021, **6**, 13310–13320.
19 Z. Fang, B. Mu, Y. Liu, N. Guo, L. Xiong, Y. Guo, A. Xia, R. Zhang, H. Zhang, R. Yao, Y. Fan, L. Li, S. Yang and R. Xiang, *Eur. J. Med. Chem.*, 2022, **255**, 115368.
20 H. Takahashi, H. Hase, T. Yoshida, J. Tashiro, Y. Hirade, K. Kitae and K. Tsujikawa, *Chem. Biol. Drug Des.*, 2022, **100**, 1–12.
21 Y. Huang, W. Xia, Z. Dong and C.-G. Yang, *Acc. Chem. Res.*, 2023, **56**, 3010–3022.
22 Y.-Z. Wang, H.-Y. Li, Y. Zhang, R.-X. Jiang, J. Xu, J. Gu, Z. Jiang, Z.-Y. Jiang, Q.-D. You and X.-K. Guo, *J. Med. Chem.*, 2023, **66**, 15944–15959.
23 T. A. Baillie, *Angew. Chem., Int. Ed.*, 2016, **55**, 13408–13421.
24 W. Chen, L. Zhang, G. Zheng, Y. Fu, Q. Ji, F. Liu, H. Chen and C. He, *FEBS Lett.*, 2014, **588**, 892–898.
25 B. Chen, F. Ye, L. Yu, G. Jia, X. Huang, X. Zhang, S. Peng, K. Chen, M. Wang, S. Gong, R. Zhang, J. Yin, H. Li, Y. Yang, H. Liu, J. Zhang, H. Zhang, A. Zhang, H. Jiang, C. Luo and C.-G. Yang, *J. Am. Chem. Soc.*, 2012, **134**, 17963–17971.
26 L. Liu, Y. Kong, L. He, X. Wang, M.-M. Wang, H. Xu, C.-G. Yang, Z. Su, J. Zhao, Z.-W. Mao, Y. Huang and H.-K. Liu, *Chin. J. Chem.*, 2022, **40**, 1156–1164; Q. Li, Y. Huang, X. Liu, J. Gan, H. Chen and C.-G. Yang, *J. Biol. Chem.*, 2016, **291**, 11083–11093.
27 T. Yang, T. Zhang, X. N. Guan, Z. Dong, L. Lan, S. Yang and C.-G. Yang, *J. Med. Chem.*, 2020, **63**, 8442–8457.
28 M. Imanishi, S. Tsuji, A. Suda and S. Futaki, *Chem. Commun.*, 2017, **53**, 12930–12933.
29 R. A. Copeland, A. Basavapathruni, M. Moyer and M. P. Scott, *Anal. Biochem.*, 2011, **416**, 206–210.
30 M. E. Flanagan, J. A. Abramite, D. P. Anderson, A. Aulabaugh, U. P. Dahal, A. M. Gilbert, C. Li, J. Montgomery, S. R. Oppenheimer, T. Ryder, B. P. Schuff, D. P. Uccello, G. S. Walker, Y. Wu, M. F. Brown, J. M. Chen, M. M. Hayward, M. C. Noe, R. S. Obach, L. Philippe, V. Shanmugasundaram, M. J. Shapiro, J. Starr, J. Stroh and Y. Che, *J. Med. Chem.*, 2014, **57**, 10072–10079.
31 L. L. Blazer, H. Zhang, E. M. Casey, S. M. Husbands and R. R. Neubig, *Biochemistry*, 2011, **50**, 3181–3192.
32 J. C. Hunter, D. Gurbani, S. B. Ficarro, M. A. Carrasco, S. M. Lim, H. G. Choi, T. Xie, J. A. Marto, Z. Chen, N. S. Gray and K. D. Westover, *Proc. Natl. Acad. Sci. U. S. A.*, 2014, **111**, 8895–8900.
33 J. M. Strelow, *SLAS Discovery*, 2017, **22**, 3–20.
34 S. Kaur, N. Y. Tam, M. A. McDonough, C. J. Schofield and W. S. Aik, *Nucleic Acids Res.*, 2022, **50**, 4148–4160.
35 J. A. Purslow, T. T. Nguyen, B. Khatiwada, A. Singh and V. Venditti, *Sci. Adv.*, 2021, **7**, eabi8215.
36 L. L. Zhou, H. Xu, Y. Huang and C.-G. Yang, *RSC Chem. Biol.*, 2021, **2**, 1352–1369; Y. Li, R. Su, X. Deng, Y. Chen and

J. Chen, *Trends Cancer*, 2022, **8**, 598–614; G.-Q. Lai, L.-L. Zhou and C.-G. Yang, *Chin. J. Chem.*, 2020, **38**, 420–421.

37 Y. Liu, G. Liang, H. Xu, W. Dong, Z. Dong, Z. Qiu, Z. Zhang, F. Li, Y. Huang, Y. Li, J. Wu, S. Yin, Y. Zhang, P. Guo, J. Liu, J. J. Xi, P. Jiang, D. Han, C.-G. Yang and M. M. Xu, *Cell Metab.*, 2021, **33**, 1221–1233; Z. Liu, Z. Duan, D. Zhang, P. Xiao, T. Zhang, H. Xu, C. H. Wang, G. W. Rao, J. Gan, Y. Huang, C.-G. Yang and Z. Dong, *J. Med. Chem.*, 2022, **65**, 10638–10654; P. Xiao, Z. Duan, Z. Liu, L. Chen, D. Zhang, L. Liu, C. Zhou, J. Gan, Z. Dong and C.-G. Yang, *J. Med. Chem.*, 2023, **66**, 9731–9752.

38 R. J. Grams and K.-L. Hsu, *Trends Pharmacol. Sci.*, 2022, **43**, 249–262.

39 J. M. Dominguez, A. Fuertes, L. Orozco, M. del Monte-Millan, E. Delgado and M. Medina, *J. Biol. Chem.*, 2012, **287**, 893–904.